13th International Workshop on Innovative Simulation for Healthcare, 011
21st International Multidisciplinary Modeling & Simulation Multiconference

2724-0371 © 2024 The Authors.
doi: 10.46354/i3m.2024.iwish.011

Stochastic modeling of glioblastoma spread: a numerical simulation study

Alessandro Borri[1,2,3], Massimiliano d'Angelo[1,2*], Laura D'Orsi[1], Marcello Pompa[1], Simona Panunzi[1] and Andrea De Gaetano[1,4,5]

[1]CNR-IASI Biomathematics Laboratory, National Research Council of Italy, Rome, Italy
[2]CNR-IASI L'Aquila Research Unit, National Research Council of Italy, L'Aquila, Italy
[3]Centre of Excellence for Research DEWS, University of L'Aquila, L'Aquila, Italy
[4]CNR-IRIB (Institute for Biomedical Research and Innovation), National Research Council of Italy, Palermo, Italy
[5]Dept. of Biomatics, Óbuda University, Budapest, Hungary

*Corresponding author. E-mail address: massimiliano.dangelo@iasi.cnr.it

Abstract

Glioblastoma, the most aggressive form of primary brain tumor, presents significant challenges in clinical management and research due to its invasive nature and resistance to standard therapies. Mathematical modeling offers a promising avenue to understand its complex dynamics and develop innovative treatment strategies. Building upon previous research, this paper reviews and adapts some existing mathematical formulations to the modeling study of glioblastoma infiltration and growth, utilizing the Partial Differential Equation (PDE) formalism to describe the time-varying and space-dependent cancer cell density. Experimental data from the literature are nicely reproduced and can be better interpreted based on the model behavior. Simulations highlight that the proposed framework is promising for further investigations.

Keywords: Tumour modeling; dynamical systems; numerical simulation; stochastic models.

1. Introduction

Glioblastoma, the most aggressive type of primary brain tumor, poses a formidable challenge in both clinical practice and biomedical research. Known for its relentless invasion of healthy brain tissue and resistance to conventional treatments, glioblastoma represents a complex interplay of genetic, molecular, and microenvironmental factors. Despite advancements in surgery, chemotherapy, and radiation therapy, the median survival for patients with glioblastoma remains dismally low, emphasizing the urgent need for innovative approaches (Wirsching and Weller, 2017).

Within the realm of mathematical modeling and simulation, glioblastoma serves as a compelling frontier, inviting researchers to explore its intricate dynamics and devise strategies to combat its formidable nature. By integrating mathematical frameworks with biological insights, researchers aim to unravel the underlying mechanisms driving glioblastoma progression, predict treatment responses, and identify novel therapeutic targets.

In this context, several authors (see e.g. Hatzikirou et al. (2005); Stein et al. (2007); Engwer et al. (2015); Conte and Surulescu (2021); Falco et al. (2021); Kumar et al. (2021); Jørgensen et al. (2023)) have developed original mathematical models of glioblastoma growth or reviewed existing ones. Among them, Stein et al. (2007),

for example, provided a new mathematical model for the increase in both invasive and central glioblastoma radius over time. Conte and Surulescu (2021) proposed multiscale modeling of glioma invasion with a focus on tissue anisotropy. In the recent review paper by Falco et al. (2021), various proposed models were explored, classified, and the significant advances of each were highlighted.

1.1. Contributions

In this work, we tackle the problem of mesoscopic mathematical modeling and simulation of glioblastoma, leveraging computational tools to dissect its complexities, as a preliminary step to pave the way for transformative interventions. By *mesoscopic* modeling we refer to capturing both the mean-field behavior (macroscopic equation) and the stochastic fluctuations of tumor behavior at the population level, rather than at the single-cell (microscopic) level (van Kampen, 2007). In particular, we build on our previous work by Pompa et al. (2023), which introduced an Agent-Based Model (ABM) simulating the infiltration of glioblastoma into the neighboring healthy brain tissue, by integrating variable cell movement and replication rates influenced by internal energy levels. We here complement the previous computational work from a more theoretical perspective, by providing some data-informed physics-based design relying on partial differential equation (PDE) modeling, representing a diffusion-reaction system, and pointing out connections with and stochastic modeling and simulation, still managing to align quantitatively with classical reported data from the literature (Stein et al., 2007). We propose alternative models for the radial position of (proliferating) tumor cells, together with a model-based characterization of the tumour core and invasion radii, by also exploiting model order reduction techniques (Borri et al., 2019) to turn the infinite-dimensional PDE systems into finite-dimensional ODE (Ordinary Differential Equation) ones, by preserving their consistency.

1.2. Organization

The paper is structured as follows. In Section 2 the mathematical tools are introduced together with the available data used in the experiments. In Section 3 the glioblastoma infiltration modeling framework is presented, while Section 4 is devoted to simulation results and their discussion. Section 5 offers concluding remarks.

2. Materials and Methods

While simplistic and restrictive, the model illustrated in this preliminary section can serve as a foundational framework for describing higher-dimensional models that exhibit certain properties of symmetry and/or isotropy, similar to those explored later in this study.

2.1. Fokker-Planck equation and the related Stochastic differential equation

Assume that, at the initial time, $t = 0$, an assembly of infinite cells are concentrated at the point $x_0 \in \mathbb{R}$. These particles promptly initiate motion, dispersing in diverse directions along erratic trajectories reminiscent of Brownian motion. Consequently, at each subsequent moment $t > 0$, we observe the particles distributed throughout space, albeit non-uniformly, governed by a probability density function (pdf), we denote by $p(t,x)$, which satisfies the following Partial Differential Equation (PDE), known as the Fokker-Planck (FP) equation:

$$\frac{\partial p(t,x)}{\partial t} = -\frac{\partial}{\partial x}\left(b(x)p(t,x)\right) + \frac{1}{2}\frac{\partial^2}{\partial x^2}\left(\sigma(x)p(t,x)\right). \quad (1)$$

The dynamical Stochastic Differential Equation (SDE) associated with the process X_t having as density the solution to (1) is given by

$$\mathrm{d}X_t = b(X_t)\,\mathrm{d}t + \sigma(X_t)\,\mathrm{d}W_t, \quad X_0 = x_0. \quad (2)$$

With the condition $\sigma^2(x) > 0$ for all x, the unique stationary solution to (1), namely $p(t,x) = \bar{p}(x)$, exists if

$$Z := \int_{-\infty}^{+\infty} \frac{1}{\sigma^2(x)} e^{2\int_0^x \frac{b(\xi)}{\sigma^2(\xi)}\,\mathrm{d}\xi}\,\mathrm{d}x < +\infty, \quad (3)$$

and is given by

$$\bar{p}(x) = \frac{1}{Z}\frac{1}{\sigma^2(x)} e^{2\int_0^x \frac{b(\xi)}{\sigma^2(\xi)}\,\mathrm{d}\xi}\,\mathrm{d}x. \quad (4)$$

We note that, if the drift term is zero, namely $b(x) = 0$, and the diffusion is still constant ($\sigma(x) = \sigma$), the process X_t in (2) is a shifted scalar Wiener process

$$dX_t = \sigma dW_t, \qquad X_0 = x_0, \quad (5)$$

which differs from the Ornstein–Uhlenbeck process (Doob, 1942) since there is no globally asymptotically stable linear drift. As a consequence, the condition (3) for the existence and uniqueness of the stationary solution fails. The solution to the Fokker-Planck equation (1), namely

$$\frac{\partial p(t,x)}{\partial t} = \frac{\sigma}{2}\frac{\partial^2}{\partial x^2}p(t,x), \quad (6)$$

is the Gaussian density

$$p(t,x) = \frac{1}{\sqrt{2\pi\sigma^2 t}} e^{-\frac{(x-x_0)^2}{2\sigma^2 t}}, \quad (7)$$

describing a continuous-time random walk with mean x_0 and variance $\sigma^2 t$, linearly increasing with time.

2.2. Data collection

In this paper we exploit the data reported by Stein et al. (2007), regarding the behavior of two different glioblastoma cell lines: U87WT and U87ΔEGFR, where the latter is a common mutation. As reported in the paper, plots of the experimental data were obtained by evaluating digital photomicrographs of the midplane of spheroids through image processing. In particular:

- the invasive radius, which represents the distance from the center of the furthest highly motile cells, is defined as the furthest distance from the center at which the gradient magnitude (averaged over the azimuthal angle) is half of its maximum value;
- the core radius, where the core represents the central part of the tumour spheroid, is instead identified as the set of pixels with an intensity of 0.12 in a scale from 0 (darkest pixel) and 1 (lighest pixel) of the gray-scale image centered on the tumor spheroid;
- the radial cell density at day 3, expressed in [cells/cm^3] is obtained directly from the dark pixel density of the digital photomicrographs.

In particular, we will try to reproduce the data in Figure 2 (panels A, B, C) in (Stein et al., 2007), namely the experimental time sequence of the invasive radius (panel A) and core radius (panel B) of the tumour from day 0 to day 7 of observations, increasing in time, and the cell density as a function of radial position at day 3 (panel C).

3. Glioblastoma infiltration modeling

We intend to utilize the technical tools introduced in the previous section to define macroscopic/mesoscopic stochastic cancer models describing the radial density/position of tumor cells and their aggregate behavior.

We build upon our preliminary agent-based model (ABM) formulation (Pompa et al., 2023), by introducing some features of interest:

- a model natively built in polar coordinates, as opposed to the Cartesian reference model (Pompa et al., 2023), (of particular interest due to the symmetry of the problem);
- by inheriting the angular (azimuthal) symmetry and isotropy of cell movements, already assumed in Pompa et al. (2023), the previous point allows to reduce the spatial dimension of the model to one (radius only); this allows to exploit and re-adapt, in part, explicit solutions and results available for 1D PDE/SDE models (see previous section);
- continuity of the model in time and space, with time/space discretization only employed for simulation purposes;
- reproduction of the behavior of two different cell lines: U87WT (already considered in CINTI) and U87ΔEGFR, which is a common mutation, for which we consider the data reported in Stein et al. (2007), see Section 2.2.

As mentioned in Section 2.2, core and invasive radii are increasing in the observation period, so a steady-state model for radial position would not be realistic. Consequently, the simplest non-stationary model we can define is the pure scalar Wiener (diffusion) process with no drift ($b(x) = 0$) and constant diffusion ($\sigma(x) = \sigma$) described in (5). By the change of coordinates $r = |x|$, from (7) one gets the half-normal density

$$p_{diff}(t,r) = \frac{\sqrt{2}}{\sqrt{\sigma^2\pi t}} e^{-\frac{r^2}{2\sigma^2 t}}, \qquad t > 0, \quad r \geq 0, \tag{8}$$

satisfying $\int_0^{+\infty} p_{diff}(t,r)dr = 1$.

In order to fit the model to the cell density radial distribution at day $t = \bar{t} = 3$ from Stein et al. (2007), which are not normalized (they are expressed in cells/cm^3), we consider the derived model

$$u_{diff}(t,r) = A \cdot p_{diff}(t,r) = \frac{A\sqrt{2}}{\sqrt{\sigma^2\pi t}} e^{-\frac{r^2}{2\sigma^2 t}}, \qquad t > 0, \quad r \geq 0, \tag{9}$$

satisfying $\int_0^{+\infty} u_{diff}(t,r)dr = A$. Notice that the model (9) does not represent a probability density function (pdf), but we assume it is equivalent to it, up to a constant ratio A.

As a comparison term, we also consider another plausible model with decreasing behavior and with the same number of free parameters (equal to 2), i.e. an exponentially decreasing function:

$$u_{exp}(r) = A \cdot p_{exp}(r) = A\lambda e^{-\lambda r}, r \geq 0, \tag{10}$$

satisfying $\int_0^{+\infty} p_{exp}(r)dr = 1$ and $\int_0^{+\infty} u_{exp}(r)dr = A$.

A refinement of the previous simplistic models would consist in adding to the FP equation (6) of the pure diffusion case a reaction term, so that the spatio-temporal evolution of the one-dimensional concentration $u(x,t)$ of tumor cells can be well described by a Reaction-Diffusion PDE, also known as KPP-Fisher Equation (see e.g. eq. (1) of Stein et al. (2007)):

$$\frac{\partial u(t,x)}{\partial t} = D\frac{\partial^2 u(t,x)}{\partial x^2} + gu(t,x)\left(1 - \frac{u(t,x)}{u_{\max}}\right), \tag{11}$$

whose solution $u_{KPP}(t,x)$ can be recast in radial coordinates by setting $r = |x|$, and where

- g is the proliferation rate;
- D is the diffusion constant;
- $u_{\max}$ is a maximum admissible concentration value, modeling intraspecific competition.

Notice that by setting $D = \frac{\sigma^2}{2}$ and $g = 0$, one easily obtains as a result the pure-diffusion density in (7). Due to the higher number of parameters (equal to four) with respect to the exponential and to the pure diffusion model, we expect that the fitted KPP-Fisher model is able to better capture the experimental tumour cell density behav-

ior. Note also that the integral $A_{KPP}(t) := \int_0^{+\infty} u_{KPP}(t,r)dr$ is non-constant, so the corresponding (normalized) pdf KPP-Fisher model can be obtained by imposing $p_{KPP}(t,r) = u_{KPP}(t,r)/A_{KPP}(t)$, so that $\int_0^{+\infty} p_{KPP}(t,r)dr = 1$.

Introducing the non-linear reaction term, we are no longer able to get an explicit solution. To this end, we exploit the multi-agent method proposed in (Borri et al., 2019) to reduce the spatially continuous PDE model into a spatially discrete one, by imposing an arbitrary space discretization $\Delta x > 0$, which leads to the following infinite ODE system:

$$\dot{u}_i(t) = \frac{D}{\Delta x^2}\left(u_{i-1}(t) - 2u_i(t) + u_{i+1}(t)\right) + g u_i(t)\left(1 - \frac{u_i(t)}{u_{\max}}\right), \tag{12}$$

for $i \in \mathbb{Z}$, where we set $u_i(t) := u_{KPP}(t, i\Delta x)$. By finite truncation of the model to the bounded set $x \in [x_{\max}, x_{\max}]$, for a proper choice of $x_{\max} > 0$, the model (12) becomes a finite ODE model, which we are able to integrate by means of standard ODE solvers.

4. Simulation results

All the computations in this section have been performed in the MATLAB® suite on a ASUS Zenbook laptop with 1.8 GHz Intel Core i7-10510U CPU and 16 GB RAM.

The ordinary least squares (OLS) method (Casella and Berger, 2024) is used to fit the parameters A and σ of the position radial density models (9) and (10), and the parameters A, σ, g and $d_{\max}$ of the KPP-Fisher model (11)–(12) to the data in Figure 2C from Stein et al. (2007), by minimizing the sum of squared differences between observed and predicted values, for both the U87WT and U87ΔEGFR cell lines, exploiting the MATLAB® routine `fminsearch`.

In Figure 1, we show the best fit of the probability density function for a fixed time $t = 3$ for the three position models proposed. It is readily seen that the half-normal model fits the data better with respect to the exponential model, approximately by a factor of 2 in terms of mean square error, for both cell lines, but both models are outperformed by the reaction-diffusion KPP-Fisher model.

After establishing the superiority of the reaction-diffusion KPP-Fisher model, namely (11), in capturing the cell density position, in Figure 2 we provide the cell density predictions in different days, where the MATLAB® routine `ode45` is employed to integrate the ODE system (12), with the choice $\Delta x = 5$ and $x_{\max} = 1000$. In this case, we do not report the normalized pdf $p_{KPP}(t,r)$ but the cell density $u_{KPP}(t,r)$ in the original coordinates, showing the progressive increase of the tumour in time and good fit the data at day 3 from Stein et al. (2007).

Instead, in Figs. 3 we provide an approximate model-based evaluation (based on the fitted KPP-Fisher model) of the invasive and core radii, evaluated in terms respectively of the 99-th and 90-th percentiles, respectively, of the

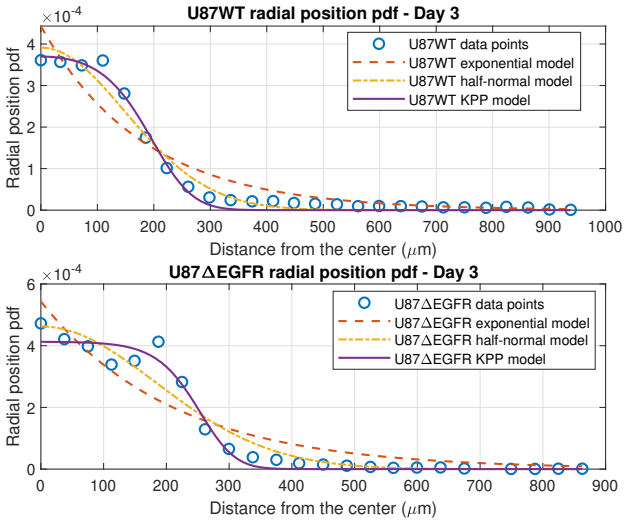

Figure 1. Best fit of the probability density function (pdf) of the radial position for the U87WT (top panel) and U87ΔEGFR cell lines at day 3: data from Stein et al. (2007) (blue circles), exponential model (red dashed line), half-normal model (yellow dash-dotted line), KPP-Fisher model (purple solid line).

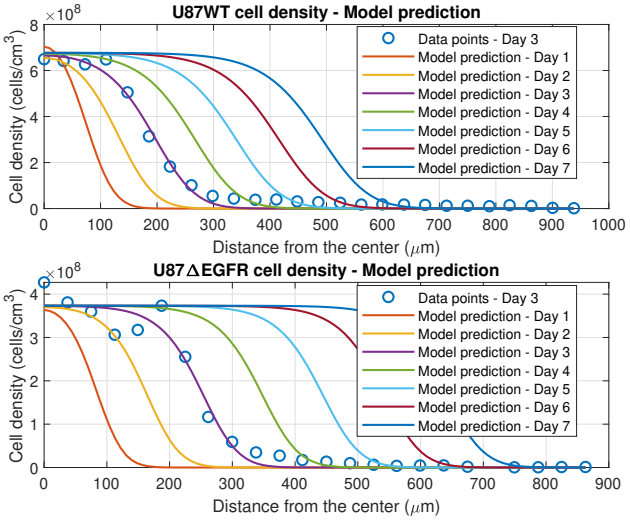

Figure 2. Predictions based on the reaction-diffusion (KPP-Fisher) model of the probability density function (pdf) of the radial position for the U87WT (top panel) and U87ΔEGFR cell lines along a period of 7 days.

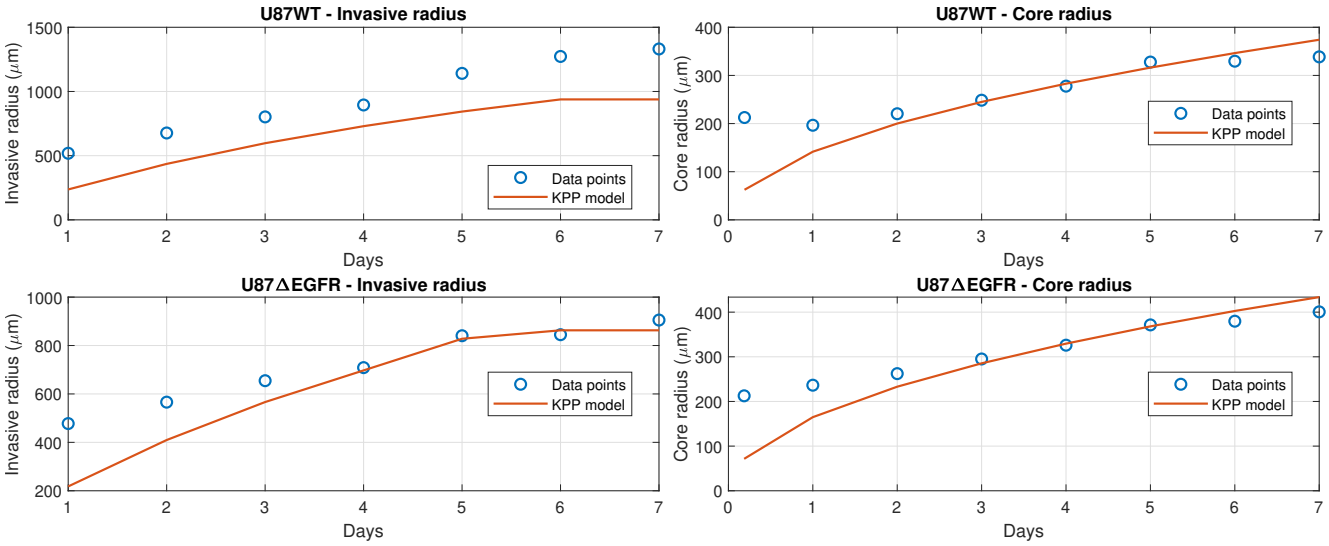

Figure 3. KPP-Fisher model evaluation of the tumour invasive radius (left figure) and core radius (right figure) along a period of 7 days for the U87WT (top panels) and U87ΔEGFR cell lines (bottom panels): data from Stein et al. (2007) (blue circles), KPP-Fisher model (red solid line).

tumour cell pdf, namely

$$\int_0^{r_{invasion}(t)} p_{KPP}(t,r)dr = 0.99, \tag{13}$$

$$\int_0^{r_{core}(t)} p_{KPP}(t,r)dr = 0.9, \tag{14}$$

where the percentile levels have been calibrated based on the available data and literature to provide reasonably good results.

Although Fig. 3 essentially captures the increasing trend in time of invasive and core radii, we highlight that the imperfect matching between the figure and the experimental data of Figures 2A–2B in (Stein et al., 2007) can easily be justified since the model has not been fitted accounting for such time-varying data from day 0 to 7, but only based on the density data at day 3. The alternative choice of fitting the KPP-Fisher model parameters based on the experimental time course of the radii, as well as the adoption of more complex models able to better capture the tumour radial expansion behavior, will be object of future investigation.

5. Conclusions

Glioblastoma poses formidable challenges in clinical practice and research, given its aggressive and treatment-resistant nature, and mathematical modeling emerges as a promising tool to comprehend the intricate dynamics of this disease and devise novel therapeutic approaches. This study contributes several innovative mathematical models for glioblastoma infiltration and growth. Leveraging the partial differential equation (PDE) formalism, we characterize the temporal and spatial variations in cancer cell density. Numerical simulations corroborate the theoretical findings and nicely replicate literature data.

The presented theoretical framework, informed by computational and data-driven approaches, seems able to offer some insights into tumor progression and potential therapeutic interventions. Regarding ongoing and future work, we highlight that the proposed design allows for versatile expansion, enabling the study of diverse cell sub-populations, tumor-immune system interactions, and personalized therapy strategies.

A. Funding

This work has been partially supported by the project "Digital Driven Diagnostics, prognostics and therapeutics for sustainable Health care" ($D^3$4-HEALTH), funded by the Italian National Recovery and Resilience Plan (NRRP) complementary fund (PNC), Next Generation EU. The work of Prof. Andrea De Gaetano was supported by the Distinguished Professor Excellence Program of Óbuda University, Budapest, Hungary.

References

Borri, A., Cusimano, V., Panunzi, S., and De Gaetano, A. (2019). Multi-agent system modeling of advection-diffusion-reaction equations. In *2019 18th European Control Conference (ECC)*, pages 2430–2435. IEEE.

Casella, G. and Berger, R. (2024). *Statistical inference*. CRC Press.

Conte, M. and Surulescu, C. (2021). Mathematical modeling of glioma invasion: acid-and vasculature mediated go-or-grow dichotomy and the influence of tissue anisotropy. *Applied Mathematics and Computation*, 407:126305.

Doob, J. L. (1942). The brownian movement and stochastic

equations. *Annals of Mathematics*, pages 351–369.

Engwer, C., Knappitsch, M., and Surulescu, C. (2015). A multiscale model for glioma spread including cell-tissue interactions and proliferation. *Mathematical Biosciences & Engineering*, 13(2):443–460.

Falco, J., Agosti, A., Vetrano, I. G., Bizzi, A., Restelli, F., Broggi, M., Schiariti, M., DiMeco, F., Ferroli, P., Ciarletta, P., et al. (2021). In silico mathematical modelling for glioblastoma: A critical review and a patient-specific case. *Journal of clinical medicine*, 10(10):2169.

Hatzikirou, H., Deutsch, A., Schaller, C., Simon, M., and Swanson, K. (2005). Mathematical modelling of glioblastoma tumour development: a review. *Mathematical Models and Methods in Applied Sciences*, 15(11):1779–1794.

Jørgensen, A. C. S., Hill, C. S., Sturrock, M., Tang, W., Karamched, S. R., Gorup, D., Lythgoe, M. F., Parrinello, S., Marguerat, S., and Shahrezaei, V. (2023). Data-driven spatio-temporal modelling of glioblastoma. *Royal Society Open Science*, 10(3):221444.

Kumar, P., Li, J., and Surulescu, C. (2021). Multiscale modeling of glioma pseudopalisades: contributions from the tumor microenvironment. *Journal of Mathematical Biology*, 82:1–45.

Pompa, M., Panunzi, S., Borri, A., and De Gaetano, A. (2023). An agent-based model of glioblastoma infiltration. In *2023 IEEE 23rd International Symposium on Computational Intelligence and Informatics (CINTI)*, pages 383–390. IEEE.

Stein, A. M., Demuth, T., Mobley, D., Berens, M., and Sander, L. M. (2007). A mathematical model of glioblastoma tumor spheroid invasion in a three-dimensional in vitro experiment. *Biophysical journal*, 92(1):356–365.

van Kampen, N. G. (2007). *Stochastic Processes in Physics and Chemistry*. 3rd Ed., The Nederlands: Elsevier.

Wirsching, H.-G. and Weller, M. (2017). Glioblastoma. *Malignant Brain Tumors: State-of-the-Art Treatment*, pages 265–288.